Fisheries and Oceans Canada | Pêches et Océans Canada
Ecosystems and Oceans Science | Sciences des écosystèmes et des océans

Canadian Science Advisory Secretariat (CSAS)

Research Document 2022/043

Ontario and Prairie Region

Recovery Potential Modelling of Lake Whitefish (*Coregonus clupeaformis*) in Lake Opeongo, Canada

Simon R. Fung, Adam S. van der Lee, and Marten A. Koops

Fisheries and Oceans Canada
Great Lakes Laboratory for Fisheries and Aquatic Sciences
867 Lakeshore Rd.
Burlington ON L7S 1A1 Canada

June 2022

Canada

Foreword

This series documents the scientific basis for the evaluation of aquatic resources and ecosystems in Canada. As such, it addresses the issues of the day in the time frames required and the documents it contains are not intended as definitive statements on the subjects addressed but rather as progress reports on ongoing investigations.

Published by:

Fisheries and Oceans Canada
Canadian Science Advisory Secretariat
200 Kent Street
Ottawa ON K1A 0E6

http://www.dfo-mpo.gc.ca/csas-sccs/
csas-sccs@dfo-mpo.gc.ca

ISSN 1919-5044
ISBN 978-0-660-43835-1 Cat. No. Fs70-5/2022-043E-PDF

Correct citation for this publication:

Fung, S.R., van der Lee, A.S., and Koops, M.A. 2022. Recovery Potential Modelling of Lake Whitefish (*Coregonus clupeaformis*) in Lake Opeongo, Canada. DFO Can. Advis. Sec. Res. Doc. 2022/043. iv + 28 p.

Aussi disponible en français :

*Fung, S.R., van der Lee, A.S., et Koops, M.A. 2022. Modélisation du potentiel de rétablissement du grand corégone (*Coregonus clupeaformis*) dans le lac Opeongo, au Canada. Secr. can. des avis sci. du MPO. 2022/043. iv + 29.*

TABLE OF CONTENTS

ABSTRACT

The Committee on the Status of Endangered Wildlife in Canada (COSEWIC) has assessed the Lake Opeongo species pair (DU 13 and 14) of Lake Whitefish (LWF, *Coregonus clupeaformis*) in Canada as Threatened. Population modelling is presented to assess the impacts of harm and determine abundance and habitat recovery targets in support of a recovery potential assessment (RPA). This analysis demonstrated that LWF populations of both DUs were most sensitive to perturbations to adult survival. Population viability analysis was used to identify potential recovery targets. Demographic sustainability (i.e., a self-sustaining population over the long term) can be achieved with adult female population sizes of ~450 to ~2,300 for the large-bodied DU or ~1,300 to ~8,700 for the small-bodied DU depending on catastrophe frequency and desired persistence probability. Lake Opeongo has sufficient habitat for populations of both DUs.

INTRODUCTION

The Lake Whitefish (LWF, *Coregonus spp.*) species complex found in Canada was evaluated by Mee et al. (2015) and 36 designatable units (DU) were recognized. Of those 36, ten DUs occur as five species pairs living within five lakes. These ten DUs were assessed by the Committee on the Status of Endangered Wildlife in Canada (COSEWIC) in 2018. The Opeongo species pair DUs (DUs 13 and 14) were assessed to be Threatened. Three other species pairs in Squanga Lake, Teslin Lake and Dezadaesh Lake (DUs 1 and 2; 3 and 4; 5 and 6) were also assessed to be Threatened. The last species pair in Como Lake (DUs 17 and 18) was assessed to be Extinct. This report will only address the DU 13 and 14 populations occupying Lake Opeongo.

The species pair in Lake Opeongo consists of a large-bodied morph (DU 14) and a small-bodied morph (DU 13). The small-bodied morph matures at an earlier age and has a shorter life-span while the large-bodied morph matures later and lives longer. Differences in body morphs for LWF may be due to difference in metabolic rate and prey availability (Trudel et al. 2001). Small morphs are generally not found when Cisco (*Coregonis artedi)* is present (Trudel et al. 2001). These morphs are typically associated with niche partitioning where the large-bodied morph is a benthic ecotype and the small-bodied morph is a limnetic ecotype. However, this association has not been established for the Opeongo LWF species pair.

Evidence for reproductive isolation between sympatric species pairs of fish has long been known for certain species such as Threespine Stickleback (*Gasterosteus aculeatus*) where mate preference (Rundle and Schluter 1998) and reduced hybrid fitness (Gow et al. 2007) discouraged interbreeding between the species pair. Mee et al. (2015) found that of the 18 LWF species pairs found across Canadian lakes, six had direct genetic evidence which supported reproductive isolation between the large-bodied and small-bodied morphs. Direct genetic analysis of the Opeongo LWF species pair to determine whether they are reproductively isolated has not yet been conducted; however, sampling and field data suggests the two DUs are reproductively isolated (Mark Ridgway, OMNRF, pers. comm.).

An alternate hypothesis is that the two DUs are not reproductively isolated but are instead two phenotypic variants of the same population. Alternative life-history strategies are frequently found among salmonids. For example, Proulx and Magnan (2004) found the benthic and pelagic polymorphism of Brook Charr (*Salvelinus fontinalis*) to be influenced by both genetic and environmental factors. Many salmonid populations often contain both migratory and resident ecotypes residing in sympatry (Jonsson and Jonsson 1993) and there is evidence that migratory ecotypes of Arctic Charr (*Salvelinus alpinus*) are not reproductively isolated (Moore et al. 2014).

While there is indirect evidence that the Opeongo LWF species pair is reproductively isolated, the morphological differences between the two DUs are also consistent with the traits that are expected to be plastic and differ between alternative life-history strategies (e.g., growth rates, age-at-maturity). In the interest of completeness and precaution, it would be prudent to consider both scenarios and ask if the uncertainty about population structure is important for the advice on how to manage Lake Whitefish in Lake Opeongo.

The *Species at Risk Act* (SARA) mandates the development of strategies for the protection and recovery of species that are at risk of extinction or extirpation from Canada. In response, Fisheries and Oceans Canada (DFO) has developed the recovery potential assessment (RPA; DFO 2007a,b) as a means of providing information and scientific advice. There are three components to each RPA: an assessment of species status, the scope for recovery, and scenarios for mitigation and alternatives to activities. This report contributes to the RPA through the use of population modelling to assess the impact of anthropogenic harm to populations and identify recovery targets for abundance and habitat with associated uncertainties. This work is

based on a demographic approach developed by Vélez-Espino and Koops (2009, 2012) and Vélez-Espino et al. (2010).

METHODS

Information on vital rates was compiled to build projection matrices that incorporate environmental stochasticity and density-dependence. The impact of anthropogenic harm to populations was quantified with the use of elasticity and simulation analyses. Estimates of recovery targets for abundance and habitat were made with estimation of the minimum viable population (MVP) and the minimum area for population viability (MAPV).

SOURCES

There is very limited published information available for the LWF species pair in Lake Opeongo. Kennedy (1943) found a bimodal distribution in the size of LWF with modes at 120 mm and 240 mm. Ihssen et al. (1981) described a relationship between fecundity and body length for Lake Opeongo LWF but did not distinguish between the two DUs.

The Ontario Ministry of Natural Resources and Forestry (OMNRF) conducted gillnet surveys in 2010, 2013 and 2018 which captured LWF of both DUs and provided DFO with a subset of their data. Individuals which were mature and smaller than 180 mm fork length were designated as belonging to the small-bodied DU while all others were designated as large-bodied DU.

All analyses and simulations were conducted using the statistical program R 3.6.3 (R Core Team 2020). Parameter values incorporated into the population model are listed in Table 1.

LIFE HISTORY

Age and Growth

Life history for the two LWF DUs differ in maximum age, maximum length and age at maturity. From the OMNRF data, the small-bodied DU begins to mature at age 2 and lives to age 8 while the large-bodied DU begins to mature at age 4 and lives to age 24. Growth differs substantially between the two DUs with the large-bodied DU having a faster growth rate and reaching greater maximum size than the small-bodied DU. Large-bodied DU length-at-age, in mm, can be described with the von Bertalanffy growth function (VBGF) as:

$$L_t = 365.4(1 - e^{-0.21(t+0.098)}) \quad (1)$$

The growth of the small-bodied DU is modelled as:

$$L_t = 142.2(1 - e^{-2.82(t+0.019)}) \quad (2)$$

The length-weight relationships for the two DUs are similar and can be modelled by:

$$W = 0.0000232L^{3.28} \quad (3)$$

Where L is fork length in mm and W is weight in grams. The growth curve and the length-weight relationship for the two DUs are depicted in Figure 1.

Table 1. Parameter definitions and values used in the population model describing LWF.

Parameter	Symbol	Description	Large-bodied DU	Small-bodied DU	Source
Age	t_{max}	Longevity	24	8	Fitted from OMNRF data
	t_{mat}	Age-at-maturity	5	2	
	ζ	Generation time	10.47	3.26	
Growth	L_∞	Asymptotic length (mm)	365.4	142.2	Fitted from OMNRF data
	k	von Bertalanffy growth coefficient	0.21	2.82	
	t_0	Age at 0 mm in length	-0.098	-0.019	
Spawning	α_f	Fecundity allometric intercept	-1.844		Ihssen et al. (1981)
	β_f	Fecundity allometric slope	2.338		
	φ	Proportion female at hatch	0.5		Assumed
	T	Spawning periodicity	1		
Weight	α_W	Length-weight allometric intercept	2.32×10^{-6}		Fitted from OMNRF data
	β_W	Length-weight allometric exponent	3.28		
Mortality	σ_a	Adult annual survival rate	0.84	0.59	Calculated
	σ_j	Juvenile survival rate	0.53-0.81	0.58	
	$\sigma_{0,1}$	Egg to age-1 survival rate at $\lambda = 1$	2.3×10^{-4}	9.3×10^{-4}	
	$\sigma_{0,max}$	Egg to age-1 survival rate at maximum λ	0.0026	0.0091	
Density-dependence	β_d	Beverton-Holt density-dependence parameter	10.32	8.75	Calculated

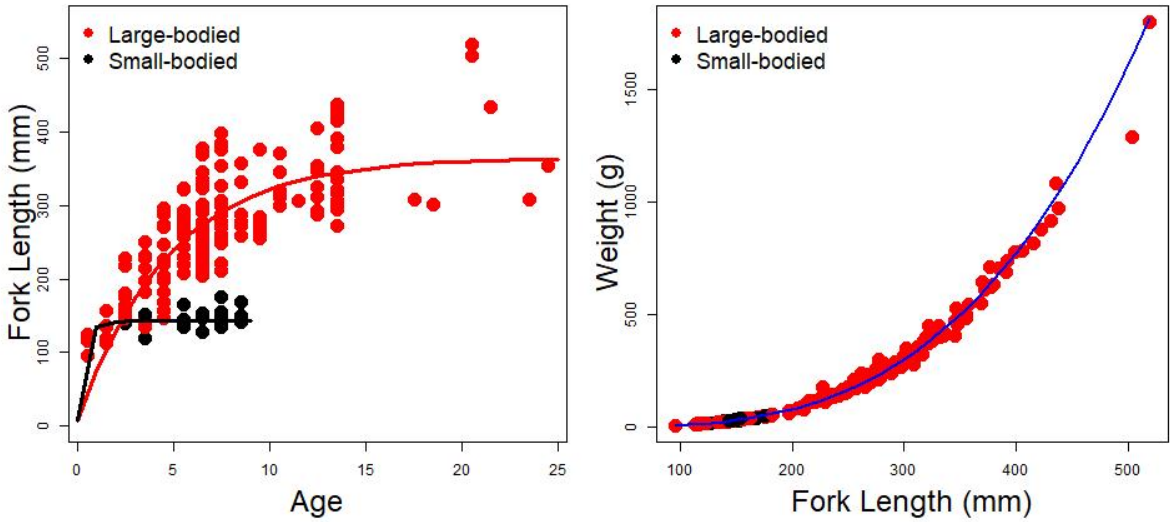

Figure 1. The von Bertalanffy growth curves for both DUs (left) and the length-weight relationship (right) for Lake Opeongo LWF. Large-bodied DU data is depicted in red while the small-bodied DU is in black. Data obtained from OMNRF.

Reproduction

Information on the length-fecundity relationship of Opeongo LWF was available from Ihssen et al. (1981), although the study did not distinguish between the two DUs. Egg counts were measured from 53 females ranging in size from 215–360 mm fork length. A relationship between length and egg count was fit as a log-transformed linear model giving the relationship:

$$\log(f) = -1.844 + 2.338 * \log(FL) \quad (4)$$

The fecundity relationship was assumed to apply to both small-bodied and large-bodied DUs. Maturity, however, differs between the large-bodied and small-bodied DUs. From examination of OMNRF data, individuals of the large-bodied DU begin reaching maturity at age 4 (24%), reach 54% mature at age 5 and become 100% mature by age 8. Small-bodied DU individuals reach 100% maturity at age 2 (Figure 2). The two DUs are difficult to distinguish when young and all individuals who mature at an early age (i.e., before age 4) were assumed to belong to the small-bodied DU while immature individuals were counted as large-bodied DU. Hence, there is a systematic bias towards undercounting immature small-bodied DU individuals and early maturing large-bodied DU individuals. A 50% sex ratio and a spawning periodicity of 1 year was assumed.

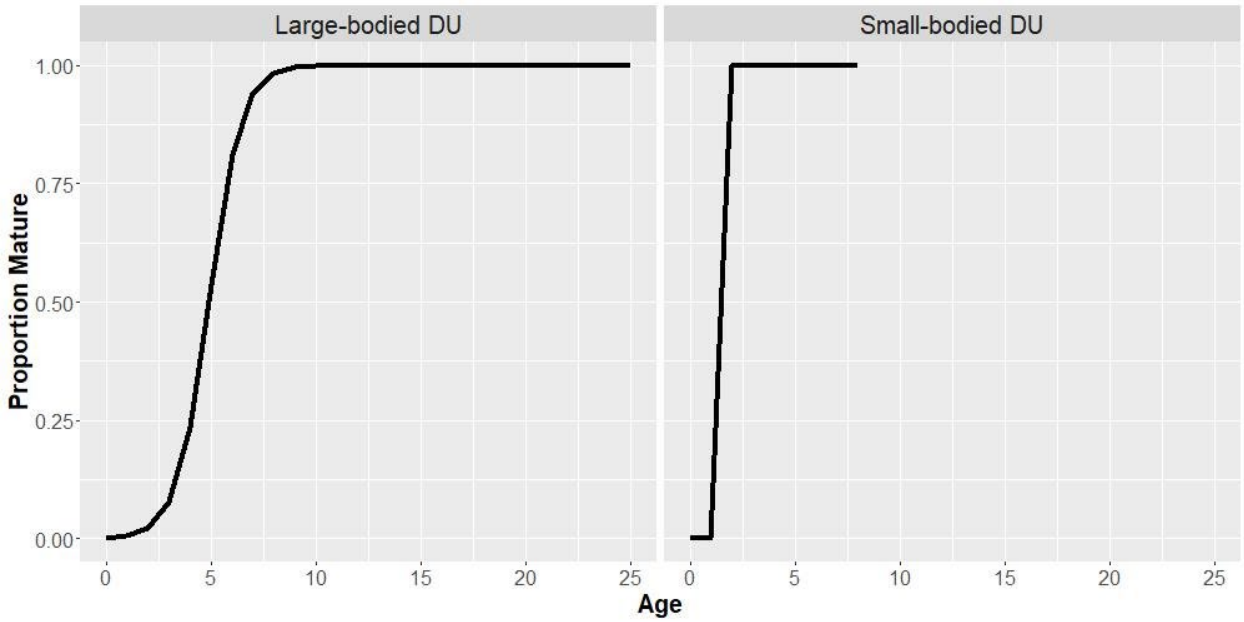

Figure 2. The proportion of mature individuals as a function of age for the large-bodied DU (left) and the small-bodied DU (right) for Lake Opeongo LWF. Data obtained from OMNRF.

Mortality

Published estimates of mortality for LWF were not available. Adult mortality for both DUs were estimated from maximum age using Hoenig's Estimator (Hoenig 1983, Kenchington 2014):

$$Z = 4.31 t_{max}^{-1.01} \quad (5)$$

Where Z is mortality and t_{max} is the maximum age. Mortality was estimated to be 0.174 and 0.528 for the large-bodied and small-bodied DUs respectively.

There was sufficient OMNRF data on the large-bodied DU to fit a catch curve which gave a mortality estimate of 0.173 for age-6 and older. There was insufficient data to fit a catch curve for the small-bodied DU, so the Hoenig estimate was relied upon.

Juvenile mortality was assumed to be greater than that of adults and increased as an inverse function of body length (Lorenzen 2000). With LWF growth described by the VBGF the mean survival rate between ages t to t+1 (σ_t) can be estimated from (van der Lee and Koops 2016):

$$\sigma_t = \left[\frac{L_t e^{-k}}{L_{t+1}}\right]^{M_r L_r / k L_\infty}. \quad (6)$$

Where k and L_∞ are VBGF parameters and M_r and L_r are mortality and length at reference size (e.g., at length-at-maturity).

To obtain the survival rate from egg to age-1, a desired level of population growth rate (λ) was first determined and then solved for the survival rate which would provide that λ given the population matrix (shown below). Young-of-Year (YOY) survival rates required for a stable population (λ = 1) and for a theoretical maximum population growth obtained from allometric relationships as presented in Randall and Minns (2000) were calculated. λ_{max} can be calculated from the maximum intrinsic rate of increase (r_{max}) where $\lambda_{max} = e^{r_{max}}$, and r_{max} can be estimated based on the productivity-weight relationship described in Randall and Minns (2000):

$$r_{max} = 2.64 W_{mat}^{-0.35} \quad (7)$$

Where W_{mat} is the weight-at-maturity in grams. This gives λ_{max} = 1.34 for the large-bodied DU and λ_{max} = 2.34 for the small-bodied DU.

THE MODEL

The LWF life cycle was modelled using a female only, density-dependent, birth-pulse, pre-breeding, age-structured population matrix model with annual projection intervals (Caswell 2001, Figure 3). To account for uncertainty in population structure, a 2-DU, interbreeding model which considered the DUs as alternative life-history strategies was developed. Offspring from both DUs are pooled into a single, undifferentiated age-1 stage which then transitions to either the large-bodied or small-bodied individuals at age 2. A parameter, *p*, determines the proportion of age-1 fish that develop into an age-2 large-bodied individuals while 1-*p* is the proportion that develop into small-bodied individuals. By setting the value of *p* to 0 or 1, the alternative life-history model simplifies into two single-DU models for the small-bodied or large-bodied DU respectively. This allows the species pair to be analyzed as either one interbreeding population with two alternative life-history strategies or two reproductively isolated DUs and to provide projections under both scenarios.

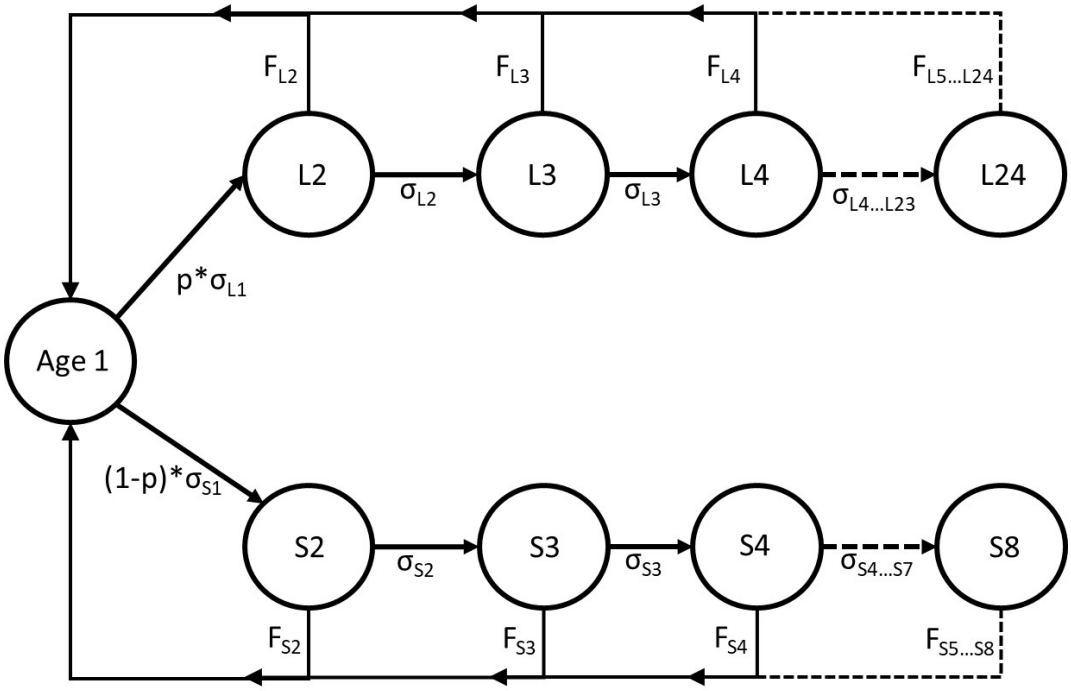

Figure 3. Generalized life cycle used to model the population dynamics of LWF. L and S denotes large-bodied and small-bodied DUs respectively. Fij represents stage-specific annual fertility of DU i and σij represents the survival from stage j to j+1 for DU i. The parameter p represents the proportion of age 1 fish which transition to large-bodied, age-2 individuals.

The matrix consisted of 31 stages (Figure 3) representing the combined age-1 of both DUs, ages 2 to 8 of small-bodied DU (denoted by S) and ages 2 to 24 of large-bodied DU (denoted by L). The projection matrix **A** is the product of the transition matrix **B**, which contains the life-history parameters, and the density-dependence matrix **D** which represents the density-dependence effects.

$$\boldsymbol{B} = \begin{bmatrix} 0 & F_{S2} & F_{S3} & F_{S4} & \cdots & F_{S8} & F_{L2} & F_{L3} & F_{L4} & \cdots & F_{L24} \\ (1-p)\cdot\sigma_{S1} & 0 & 0 & 0 & \cdots & 0 & 0 & 0 & 0 & \cdots & 0 \\ 0 & \sigma_{S2} & 0 & 0 & \cdots & 0 & 0 & 0 & 0 & \cdots & 0 \\ 0 & 0 & \sigma_{S3} & 0 & \cdots & 0 & 0 & 0 & 0 & \cdots & 0 \\ \vdots & \vdots & \vdots & \vdots & \ddots & \vdots & \vdots & \vdots & \vdots & \ddots & \vdots \\ 0 & 0 & 0 & 0 & \cdots & 0 & 0 & 0 & 0 & \cdots & 0 \\ p\cdot\sigma_{L1} & 0 & 0 & 0 & \cdots & 0 & 0 & 0 & 0 & \cdots & 0 \\ 0 & 0 & 0 & 0 & \cdots & 0 & \sigma_{L2} & 0 & 0 & \cdots & 0 \\ 0 & 0 & 0 & 0 & \cdots & 0 & 0 & \sigma_{L3} & 0 & \cdots & 0 \\ 0 & 0 & 0 & 0 & \cdots & 0 & 0 & 0 & \sigma_{L4} & \cdots & 0 \\ \vdots & \vdots & \vdots & \vdots & \ddots & \vdots & \vdots & \vdots & \vdots & \ddots & \vdots \\ 0 & 0 & 0 & 0 & \cdots & 0 & 0 & 0 & 0 & \cdots & 0 \end{bmatrix} \quad (8)$$

and:

$$\mathbf{A} = \mathbf{B} \circ \mathbf{D}, \quad (9)$$

where the symbol ∘ represents the Hadamard product or the element by element multiplication of the matrices.

The age-based matrix model incorporated the fertility parameter F_{ij}, and the annual survival rate σ_{ij}, with the subscript *i* denoting the DU type and the subscript *j* representing the age. Fertility, F_{ij}, is the product of all reproductive parameters and as a pre-breeding matrix also incorporates the probability of surviving from the egg stage to age-1 (σ_0):

$$F_{ij} = {}^{f_{ij}\varphi m_{ij}\sigma_{0,1}}/_{T} \quad (10)$$

Where f_{ij} represents age-specific fecundity of DU *i* at age *j*, φ represents the sex ratio, m_{ij} represents the proportion of mature females of DU *i* at age *j*, $\sigma_{0,1}$ represents survival from egg to age-1 under stable population growth, and T represents spawning periodicity which was assumed to be 1 year.

Density-dependence

Density dependence was assumed to only act on the first year of life. Density-dependence was incorporated using the Beverton-Holt (Equation 11) function. The function was adapted to the density-dependence matrix **D** which when multiplied by the equilibrium egg-to-age-1 survival rate $\sigma_{0,1}$ would produce the equilibrium rate when egg production is at carrying capacity and would approach the maximal survival rate $\sigma_{0,max}$ as egg production approaches 0 (Equation 12).

$$R = \frac{\alpha N}{1+\beta N} \quad (11)$$

$$d_0 = \frac{{}^{\sigma_{0,max}}/_{\sigma_{0,1}}}{1+\beta_d \frac{N_e}{K_e}} \quad (12)$$

Where $\sigma_{0,max}$ and $\sigma_{0,1}$ represent maximum and equilibrium egg-to-age-1 survival rates respectively. β_d is the density-dependence parameter scaled to a single individual and is equivalent to $\frac{\sigma_{0,max}}{\sigma_{0,1}} - 1$. N_e is the current annual egg production and K_e is egg production at carrying capacity.

The density-dependence matrix **D** was structured as shown below and is of the same size as the transition matrix **B**.

$$\mathbf{D} = \begin{bmatrix} 1 & d_0 & d_0 & d_0 & \cdots & d_0 \\ 1 & 1 & 1 & 1 & \cdots & 1 \\ 1 & 1 & 1 & 1 & \cdots & 1 \\ 1 & 1 & 1 & 1 & \cdots & 1 \\ \vdots & \vdots & \vdots & \vdots & \ddots & \vdots \\ 1 & 1 & 1 & 1 & \cdots & 1 \end{bmatrix} \quad (13)$$

Stochasticity

Fertility and age-specific survival were varied annually to simulate environmental stochasticity in vital rates. Based on analyses of the length-fecundity relationship of LWF populations from a Great Lakes LWF database, the intercept of the allometric fecundity relationship (Equation 4) was assumed to follow a normal distribution around the mean value with a coefficient of variation (CV) of 0.02. This translates to an egg count CV of ~0.08. This assumes that environmental stochasticity affects the elevation of the length-fecundity relationship but the effect of body size on fecundity is unaffected by inter-annual variability in environmental conditions.

Age-specific survival was assumed to follow a lognormal distribution. Survival rate was varied as instantaneous mortality ($\sigma_{ij} = e^{-M_{ij}}$). *M* was assumed to vary following a normal distribution with a CV of 0.1 for (YOY) and 0.15 for juveniles and adults. Stochasticity was executed using the stretched-beta distribution to remove the extreme tails of the normal distribution but maintain the mean and standard deviation (Morris and Doak 2002). To account for similarities in mortality experienced by individuals of similar age, *M* was assumed to correlate between age classes of the same DU with an AR1 correlation structure (correlation diminishes as difference between ages increases) with a correlation value of 0.75. Correlation between age classes of different DUs was assumed to be 0.25. YOY survival was assumed to vary independently of the older stages (correlation = 0).

IMPACT OF HARM

The impact of anthropogenic harm to the Opeongo LWF population was assessed with deterministic elasticity analyses of the projection matrix and stochastic simulations.

Elasticity analysis is a method to quantify the impact of changes of vital rates on a population. The elasticity value represents the proportional change to the population growth rate (λ) from a proportional change in a vital rate. For example, an elasticity value of 0.1 for fertility would indicate that the population growth rate would increase by 1% if fertility increased by 10%.

Elasticities are useful as they allow for assessment of how impactful changes to vital rates and other model parameters are to a population. Because they represent proportional changes their values are directly comparable. They are preferable to simulation analyses because of the speed with which they can be estimated allowing for many more perturbations to be examined than simulations. Elasticities are limited, however, as they represent permanent changes and assume all other model parameters remain unchanged. As a result, simulation analysis was used to examine the effects of transient or periodic harm to a population.

Elasticity of λ

Elasticities of λ (ε_λ) are calculated by taking the scaled partial derivatives of λ with respect to a vital rate (ν, Caswell 2001):

$$\varepsilon_\lambda = \frac{\nu}{\lambda}\sum_{i,j}\frac{\partial\lambda}{\partial a_{i,j}}\frac{\partial a_{i,j}}{\partial \nu}, \quad (14)$$

where a_{ij} is the projection matrix element in row *i* and column *j*.

Elasticity estimates are influenced by current conditions and elasticity analysis was performed for four states of population growth: declining, stable, growing and booming. A declining population was defined based on COSEWIC criterion A2 for Threatened species: a ≥ 30% reduction in population size over 10 years or 3 generation, whichever is longer. This gives a λ_{min} = 0.989 for the large-bodied DU. For the small-bodied DU, since 10 years is longer than 3 generations, the rate was calculated based on a 10-year decline which gives λ_{min} = 0.965. A stable population is defined as one with λ_1 = 1. A booming population was one with the population growth rate at the maximum value estimated using Equation 7, which was λ_{max} = 1.34 for the large-bodied DU and λ_{max} = 2.34 for the small-bodied DU. Finally, a growing population was defined as the geometric mean of λ_1 and λ_{max} and thus λ_{grow} is equal to 1.16 for the large-bodied DU and 1.53 for the small-bodied DU.

For the 2-DU, alternative life-history model where the proportion of large-bodied DU is determined by the *p* parameter, λ_{max} is the *p*-weighted mean of the λ_{max} of the two DUs. λ_{grow} is then calculated from λ_{max} as above. Generation times and λ values are listed in Table 2.

Table 2. Generation times and growth rates (declining, stable, growing and booming) for the small-bodied DU, the large-bodied DU and the alternative life-history population at various proportions of the large-bodied DU. λ_{min} produces a 30% decline over 3 generations or 10 years, whichever is longer.

Proportion of Large-bodied DU (*p*)	Generation Time	Growth Rates			
		Declining (λ_{min})	Stable (λ_1)	Growing (λ_{grow})	Booming (λ_{max})
0 (Small-bodied DU only)	3.26	0.965	1	1.53	2.34
0.1	5.47	0.978	1	1.5	2.24
0.25	7.37	0.984	1	1.44	2.09
0.5	9.02	0.987	1	1.36	1.84
0.75	9.91	0.988	1	1.26	1.59
0.9	10.27	0.988	1	1.2	1.44
1 (Large-bodied DU only)	10.47	0.989	1	1.16	1.34

Simulation

Simulation analysis was used to investigate the impacts of stage-specific harm on adult population density. Stage-specific survival rates were reduced by some level of harm, ranging from 0 to 99% in intervals of 10%. This harm was applied at different frequencies (once every 1, 2, 5 and 10 years) over a 100 year simulation period. A frequency of 1 indicates that harm is constant and applied every year, whereas a frequency of 10 indicates that harm is periodic and applied once every 10 years. To measure harm, the mean population size over the last 15 years of simulation was divided by the initial carrying capacity, resulting in a proportion of *K*. As a

density-dependent model, it is assumed for simulations where harm intervals are greater than one year that the population is able to recover in between applications of harm as conditions are returned to the initial state.

RECOVERY TARGETS

Abundance: Minimum Viable Population (MVP)

The concept of demographic sustainability was used to identify potential minimum recovery targets for LWF. Demographic sustainability is related to the concept of a minimum viable population (MVP, Shaffer 1981), and was defined as the minimum adult population size that results in a desired probability of persistence over 100 years, where 'adult' corresponds to mature females. MVP was estimated using simulation analysis which incorporated environmental stochasticity and density-dependence.

Important elements incorporated in population viability analysis include: the choice of time frame over which persistence is determined, the severity and frequency of catastrophic events, and the quasi-extinction threshold below which a population is deemed unviable. The choice of time frame is arbitrary and without biological rational; however, 100 years is likely reasonable for making management decisions.

The rate and severity of catastrophic events within LWF populations is unknown. Based on a meta-analysis, Reed et al. (2003) determined that among vertebrate populations, catastrophic die-offs that resulted in a one-year decrease in population size > 50% occurred at a rate of 14% per generation on average. This result was used to guide the MVP simulations and 2 levels of catastrophe rate were used to allow for uncertainty: 10% per generation and 15% per generation. Since the generation time for the two DUs are different, separate annual catastrophe rates were computed for the two DUs. These rates correspond to an annual catastrophe probability of 1% and 1.7% for the large-bodied DU and an annual probability of 3.3% and 5.2% for the small-bodied DU. For the alternative life-history model, generation time and annual catastrophe rate are affected by the parameter *p* and for values between 0 and 1, generation times and annual catastrophe rates are intermediate between the value for the two DUs.

The impact of catastrophes affect all life-stages simultaneously and was drawn randomly from a beta distribution scaled between 0.5 and 1 with shape parameters of 0.762 and 1.5 (Reed et al. 2003; Figure 4), representing the probability of a 50 to 100% decline in population size. Catastrophes represent any temporary and reversible large-scale disturbance to the population and may be from natural or anthropogenic causes.

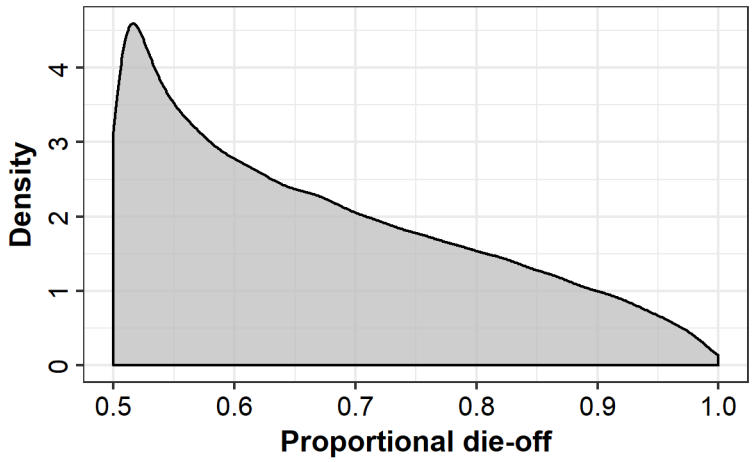

Figure 4. Beta distribution (scaled between 0.5 and 1) used in stochastic draws of catastrophic impacts. This represents the proportional decrease in population size following a catastrophic event. Shape parameters were 0.762 and 1.5 (Reed et al. 2003).

Quasi-extinction accounts for the compounding effects of Allee effects, demographic stochasticity and inbreeding depression (Lande 1988) leading a population to extinction once the threshold is crossed. The value of the quasi-extinction threshold cannot be empirically measured; therefore, 25 adult females was used as a reasonable approximation (Morris and Doak 2002).

Density-dependent, stochastic simulations were conducted for populations of various initial densities (initial density represented adult female carrying capacity, K_a, where λ = 1). Simulations were run for 100 years. Independent simulations incorporated two rates of catastrophes (0.1 and 0.15 per generation). Each simulation was replicated 5,000 times and the number of quasi-extinctions were counted. The probability of extinction (*P[ext.]*) was modelled as a logistic regression, such that:

$$P[ext.] = \frac{1}{1+e^{-(b_{MVP} log_{10}(N_a)+a_{MVP})}}, \quad (15)$$

where a_{MVP} and b_{MVP} represent the fitted intercept and slope from the logistic regression. Equation 15 can be rearranged to estimate the adult population size required to give a desired level of population persistence (MVP):

$$MVP = 10^{-\frac{\log\left(1/P[ext.]-1\right)+a_{MVP}}{b_{MVP}}}. \quad (16)$$

MVP estimates are presented for quasi-extinction probabilities of 5% and 1%.

Habitat: Minimum Area for Population Viability (MAPV)

Minimum area for population viability (MAPV) is defined as the quantity of habitat required to support a population of MVP size (Velez-Espino et al. 2010). MAPV is estimated simply as MVP divided by mean population density. Large-bodied DU population estimates were available from OMNRF for 2010 and 2019 and mean density could be calculate from those estimates by dividing the population estimate by the lake surface area. Small-bodied DU population estimates were not available and the equation from Table 2 of Randall et al. (1995) was used to provide a density estimate:

$$\log D = 4.48 - 1.01 * \log W \quad (17)$$

Where D is the number of individuals per hectare and W is the mean weight of the fish in grams. To adjust Equation 17 to more accurately reflect the LWF population in Lake Opeongo, the intercept was scaled such that the equation would produce the OMNRF density estimate for the large-bodied DU. The intercept-adjusted equation was then used to estimate the density of the small-bodied DU. The use of the entire lake area in these calculations could be justified in that the entire lake contributes to the productivity even if LWF doesn't necessarily occupy the entire lake.

RECOVERY TIMES

Time to recovery was estimated using simulation analysis similar to MVP simulations. Simulations began with initial population sizes set to 10% of MVP. Simulations incorporated: stochasticity, density-dependence, and catastrophes in the same manner as MVP simulations. The population was deemed recovered when MVP was reached (MVP was also used as carrying capacity). Simulations were repeated 5,000 times. Setting carrying capacity at MVP can be viewed as the minimum population size necessary for population persistence. This assumption would result in the longest times for recovery for a viable population. If carrying capacity were greater than MVP, recovery times would be shorter.

RESULTS

IMPACT OF HARM

The impact of harm to LWF populations were analyzed with deterministic elasticity analysis on the population growth rate and with population simulations.

Elasticity of λ

The elasticity of λ to perturbations of vital rates gives an indication of how the population may respond to changes in vital rates; positive values indicate that population growth rate will increase if the vital rate is increased. Elasticity estimates are presented for fertility (F) which encompasses all parameters contributing to Equation 10 and survival rates (σ) for the YOY, juvenile, and adult stages. Figure 5 shows the results for when the two DUs are considered as separate populations and Figure 6 shows the results for five different values of p for when the two DUs are considered alternative life-histories.

In general, sensitivity to changes in vital rates is dependent on the population's current growth rate. For the large-bodied DU, adult survival has the strongest effect for populations at stable or declining growth rates while at growing or booming growth rates, λ becomes more sensitive to juvenile survival. Fertility and YOY survival elasticity value increases slightly from ~0.1 at declining and stable growth rates to ~0.15 at growing or booming growth rates.

The small-bodied DU exhibit a similar pattern of elasticity being dependent on current growth rates. Adult survival has the strongest effect at declining or stable population growth rates and decreases as growth rate increases. Fertility, YOY and juvenile survival have similar elasticity values which increase from ~0.3 to ~0.43 as growth rate increases.

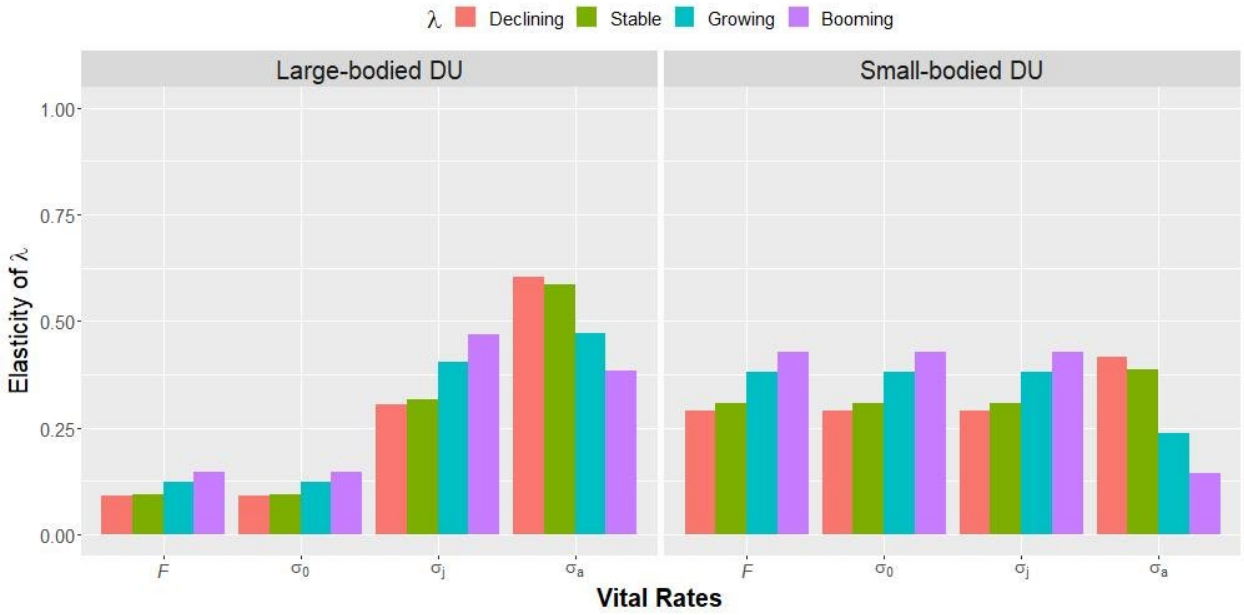

Figure 5. Elasticity of λ analysis for separate Large-bodied and Small-bodied DU models under 4 population growth states: declining, stable, growing and booming. F represents fertility indicating the effects of independent perturbations to all parameters that contribute to fertility (Equation 10) and σ represents survival for the YOY (0), juvenile (j) and adult (a) stages.

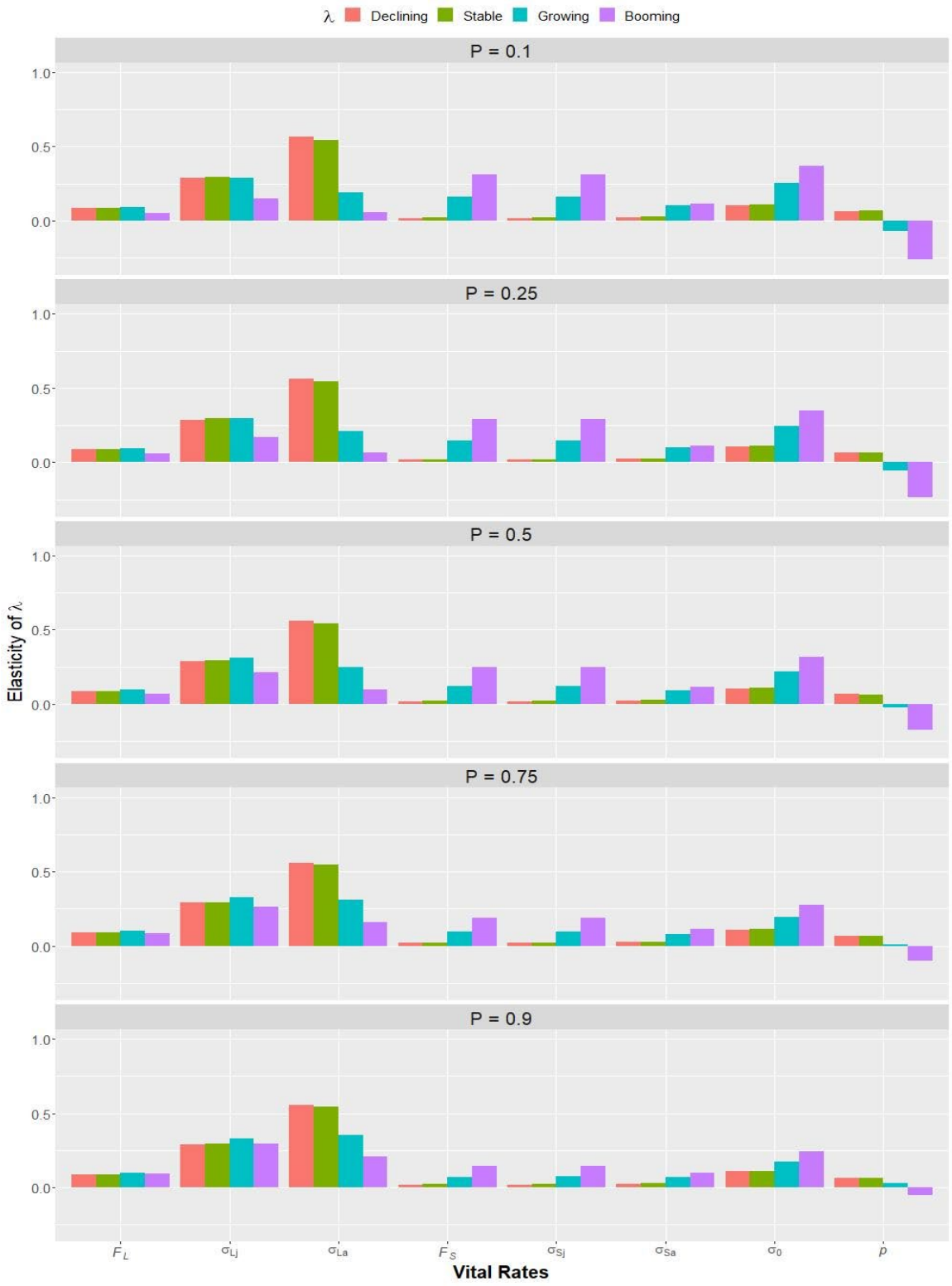

Figure 6. Elasticity of λ analysis for the alternative life-history population model under 5 levels of p and 4 population states: declining, stable, growing and booming. F_L, σ_{Lj} and σ_{La} represents fertility, juvenile survival and adult survival respectively for the large-bodied DU. F_S, σ_{Sj} and σ_{Sa} represents fertility, juvenile survival and adult survival respectively for the small-bodied DU. σ_0 represents YOY survival and p represents the proportion of age-1 fish which develop into age-2 large-bodied individuals.

The elasticity analysis results for the alternative life-history model are generally similar across all five values of *p* examined and depends on the current growth rate. Population growth rate is most sensitive to large-bodied adult and juvenile survival rates at stable or declining populations. At growing or booming growth rates, small-bodied vital rates (fertility, juvenile and adult survivals) exert a stronger impact. The proportion of large-bodied individuals, *p*, exhibits the most variable effect on λ as it switches from a positive to negative elasticity value as growth rate increases. This means that for λ below a certain threshold, an increase in the proportion of large-bodied individuals would provide an increase to the overall population growth rate whereas above that threshold, growth rate is increased by increasing the proportion of small-bodied individuals.

Simulation

The above elasticity analyses assume that any change to a vital rate is permanent. Therefore, simulation analysis was used to investigate how adult population size may respond to periodic perturbations occurring annually (for comparison to elasticity analysis), every second year, fifth year, and tenth year. The simulations were performed on a large-bodied DU model, a small-bodied DU model and an alternative life-history model with *p* at 0.5 (Figure 7, 8 and 9 respectively). For the large-bodied and small-bodied DU reproductively isolated populations, harm was applied to either the YOY stage or the combined juvenile and adult stages. For the alternative life-history population, harm was applied to the YOY stage, the juveniles and adults of the small-bodied DU, the juveniles and adults of the large-bodied DU or all the juveniles and adults.

The population reduction as a result of harm has a large confidence interval likely due to high stochasticity in vital rates. However, despite the large confidence intervals, the overall pattern displayed by the simulations is consistent with the elasticity analysis.

Figure 7 and 8 depicts the impact of harm to reproductively isolated DUs and the population is scaled to reflect only the population of that DU. For both DUs, the impact of harm is greater when it's applied to the juvenile and adult stages than the YOY stage. The population trajectory has a more negative slope when harm is applied to juveniles and adults and reaches extinction at lower levels of harm.

Figure 9 depicts harm to an interbreeding population and the population is scaled to reflect the sum of the population of both DUs. Figure 10 shows the realized proportion of the large-bodied DU when harm is applied. For the alternative life-history model, the impact of harm is greater when it's applied to the juvenile and adults of the large-bodied DU than when applied to the small-bodied DU. This is also consistent with the elasticity analysis. Harm to adults and juveniles of the large-bodied DU also has a greater initial rate of population reduction than harm to YOY. Harm applied to either of the DUs alone cannot drive the entire population to extinction regardless of the level of harm; this requires harm to be applied to juveniles and adults of both DUs or to the YOY stage for extinction. However, harm to a single DU can essentially eliminate that DU from the population (Figure 10). Considering a population with $p = 0.5$ (Figure 9), applying harm to a single DU which comprises approximately half of the population can reduce the total population down to 50% of the carrying capacity, through the elimination of that DU from the population. This is more likely to happen through the application of harm to the large-bodied DU, consistent with the higher elasticities for adult and juvenile stages of the large-bodied DU.

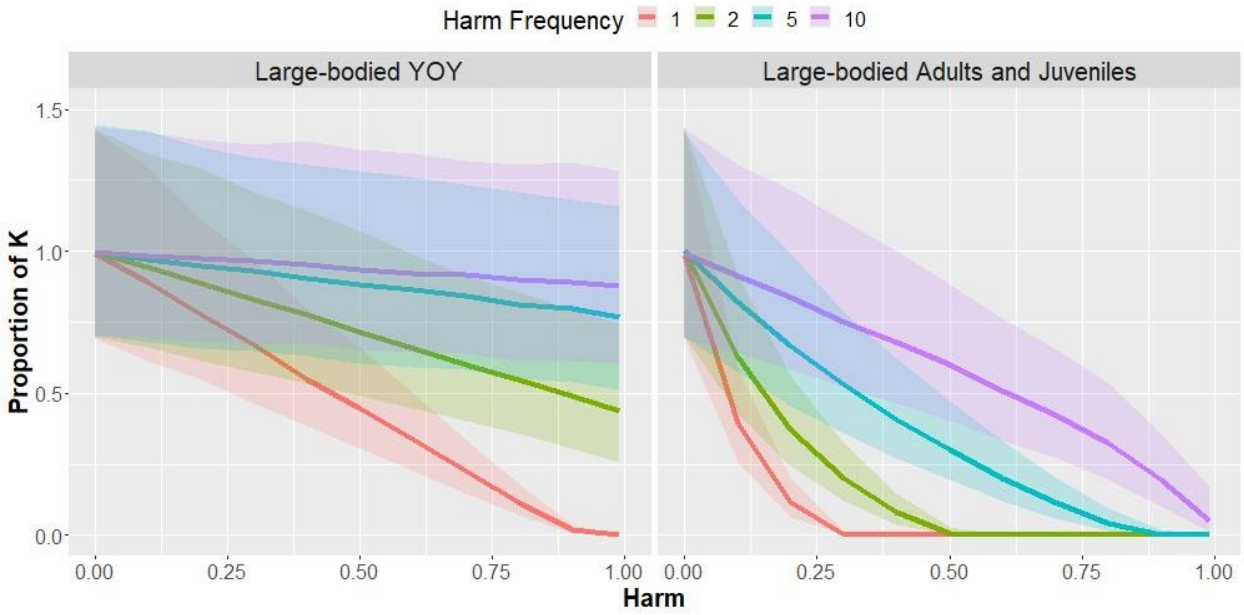

Figure 7. Results from harm simulation analysis where harm is applied at different frequencies to either the YOY or the age-1 and older for the large-bodied DU. The x-axis represent the proportional harm (e.g., annual mortality) applied to the life-stage and the y-axis represents the proportional decrease in large-bodied DU adult abundance in the final 15 years of a 100 year simulation. The solid lines represent the median impact and the surrounding polygons represent 95% confidence intervals.

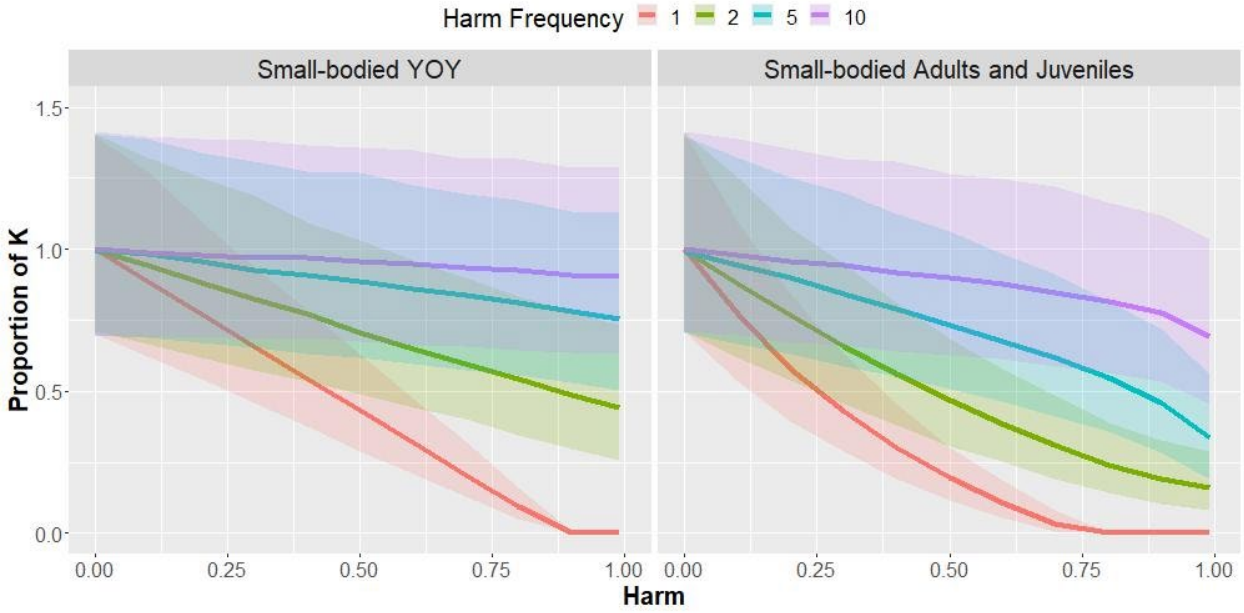

Figure 8. Results from harm simulation analysis where harm is applied at different frequencies to either the YOY or the age-1 and older for the small-bodied DU. The x-axis represent the proportional harm (e.g., annual mortality) applied to the life-stage and the y-axis represents the proportional decrease in small-bodied DU adult abundance in the final 15 years of a 100 year simulation. The solid lines represent the median impact and the surrounding polygons represent 95% confidence intervals.

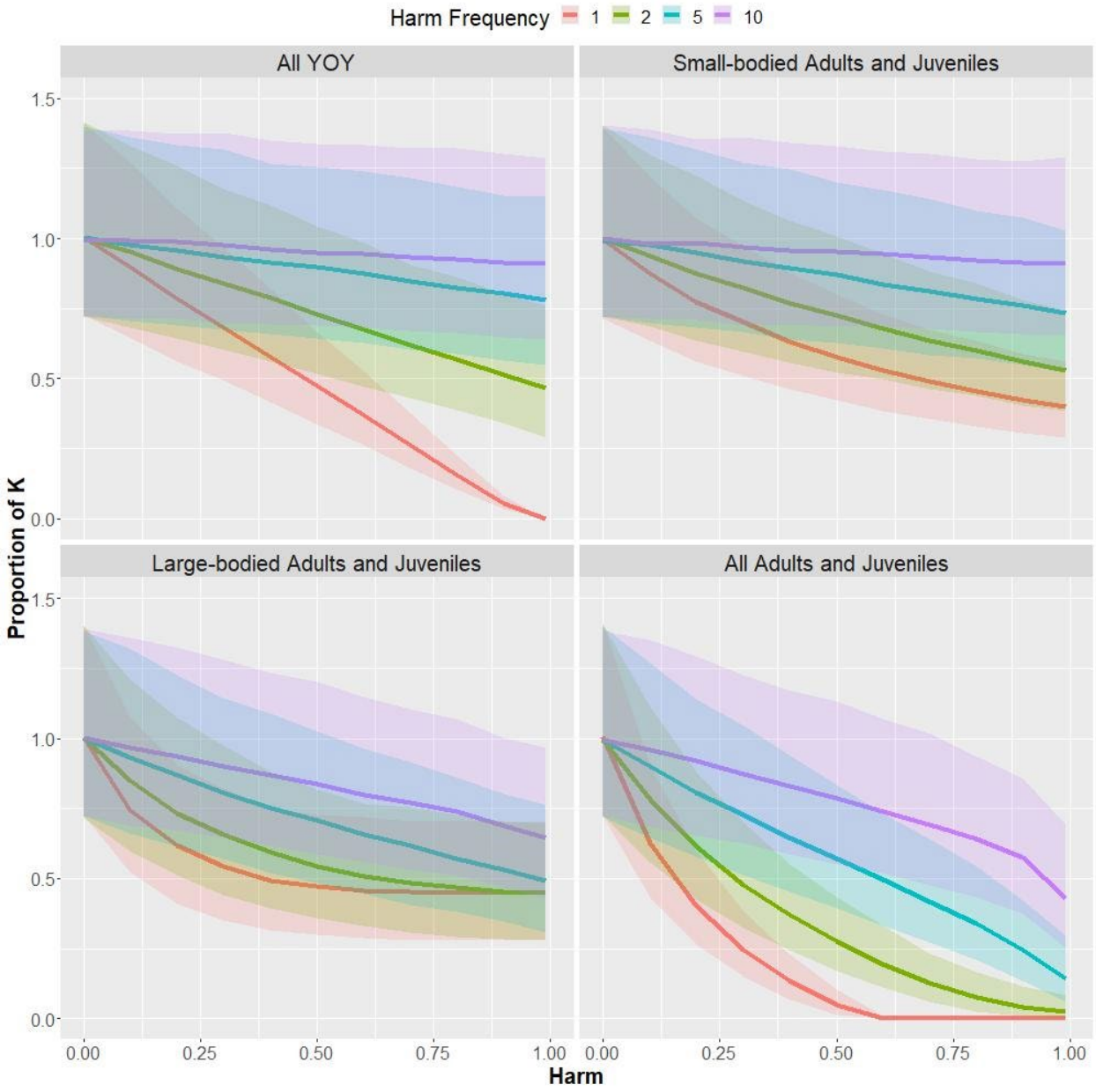

Figure 9. Results from harm simulation analysis where harm is applied at different frequencies to specific life-stages in the alternative life-history model. The x-axis represent the proportional harm (e.g., annual mortality) applied to the life-stage and the y-axis represents the proportional decrease in combined adult abundance in the final 15 years of a 100 year simulation. The solid lines represent the median impact and the surrounding polygons represent 95% confidence intervals. The population values in this figure represents the combined population of both large-bodied and small-bodied DUs. In the Small-bodied Adults and Juveniles panel and the Large-bodied Adults and Juveniles panel, harm is being applied to only one DU, hence the population as a whole cannot be driven to extinction. However, the region where the line flattens essentially represent the extinction of the DU being harmed.

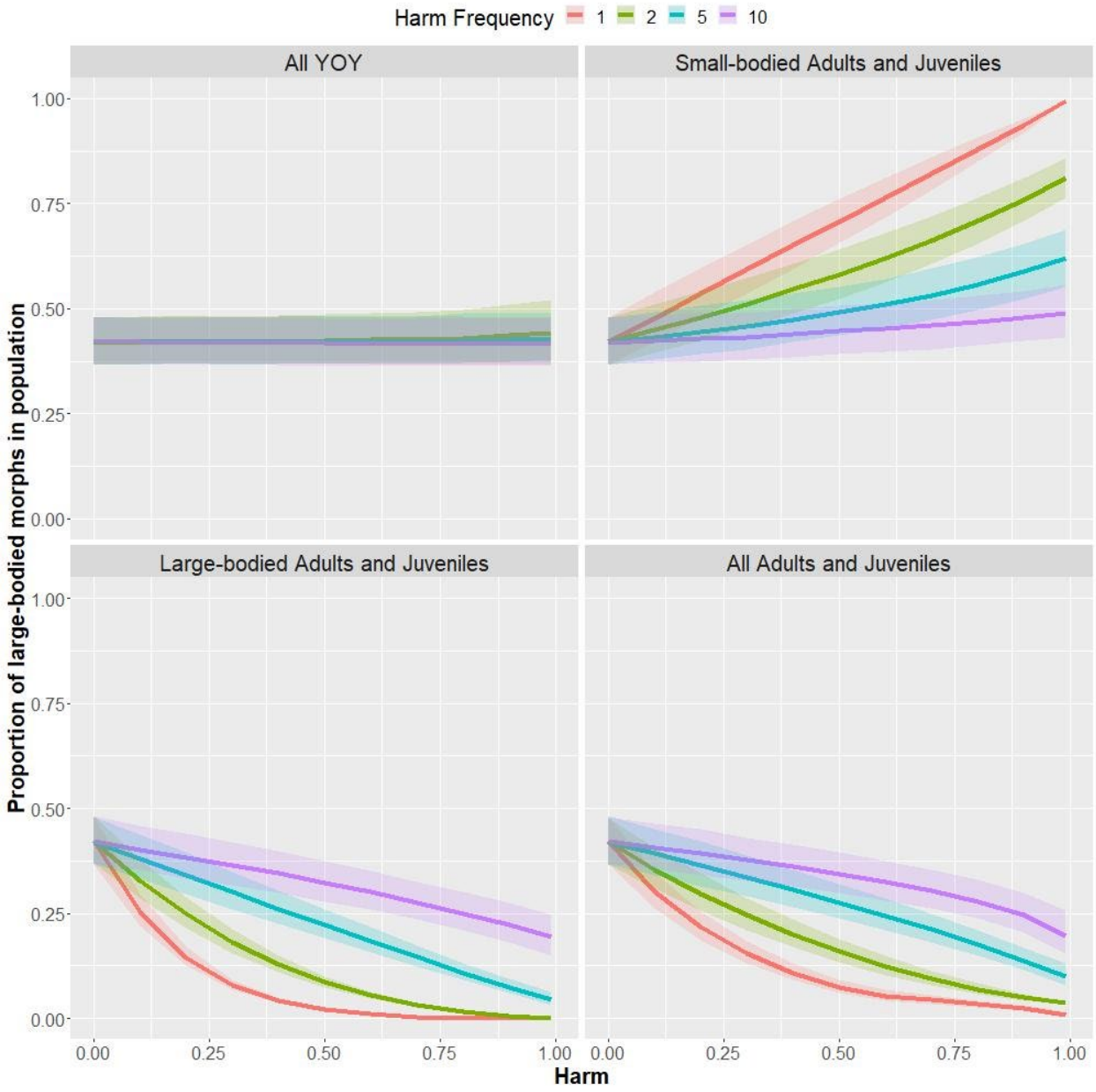

Figure 10. Results from harm simulation analysis where harm is applied at different frequencies to specific life-stages in the alternative life-history model. The x-axis represent the proportional harm (e.g., annual mortality) applied to the life-stage and the y-axis represents the realized proportion of the large-bodied DU in the population in the final 15 years of a 100 year simulation. The solid lines represent the median proportion and the surrounding polygons represent 95% confidence intervals. When harm is applied to the small-bodied DU (Small-bodied Adults and Juveniles panel), the proportion of large-bodied DU increases. When harm is applied to the large-bodied DU (Large-bodied Adults and Juveniles panel), the proportion of large-bodied DU decreases. As the level of harm increases, the proportion moves towards either 0 or 1, at which point one of the DUs essentially become extinct.

RECOVERY TARGETS

Abundance: Minimum Viable Population (MVP)

Demographic sustainability was assessed using stochastic, density-dependent population simulations. Simulation outputs (the proportion of simulations reaching the threshold for quasi-extinctions) were fitted using a logistic regression (Table 3; Figure 11 and 12).

Recovery target abundances that provide a 5% and 1% probability of quasi-extinction over 100 years are presented (Table 4). Simulation outputs applied solely to adult females in the population and should be doubled to obtain whole adult (male and female) population estimates.

Table 3. Parameter values from logistic regression of extinction probability and adult female population size for LWF population.

Proportion of Large-bodied DU (*p*)	10% Catastrophe Rate per Generation		15% Catastrophe Rate per Generation	
	a_{MVP}	b_{MVP}	a_{MVP}	b_{MVP}
0 (Small-bodied DU Only)	7.350	-3.303	7.361	-3.035
0.1	7.133	-3.483	7.034	-3.208
0.25	7.245	-3.694	7.087	-3.391
0.5	6.656	-3.591	6.708	-3.373
0.75	6.281	-3.504	6.965	-3.526
0.9	6.347	-3.562	6.724	-3.425
1 (Large-bodied DU only)	6.062	-3.400	6.543	-3.313

Table 4. The number of adult females for LWF minimum viable population (MVP) under two catastrophe rates and for two probabilities of quasi-extinction.

Proportion of Large-bodied DU (*p*)	10% Catastrophe Rate per Generation		15% Catastrophe Rate per Generation	
	5% Risk of Extinction	1% Risk of Extinction	5% Risk of Extinction	1% Risk of Extinction
0 (Small-bodied DU only)	1309	4137	2489	8709
0.1	782	2327	1290	4217
0.25	574	1606	909	2786
0.5	472	1358	728	2245
0.75	430	1271	647	1900
0.9	407	1182	665	2017
1 (Large-bodied DU only)	446	1363	731	2302

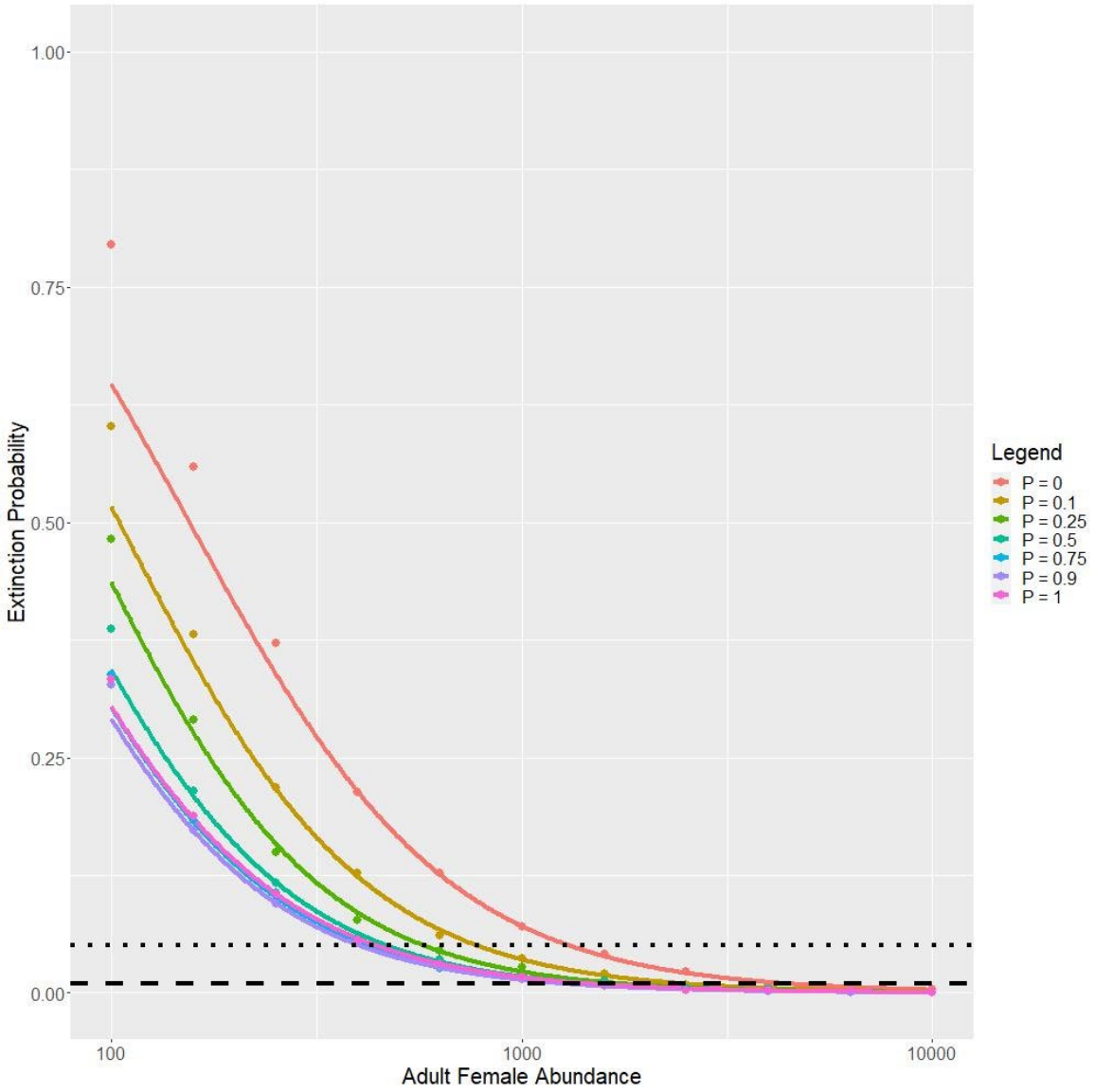

Figure 11. The probability of quasi-extinction at various adult female abundances for seven large-bodied DU proportions and at a 10% per generation catastrophe rate. The points represent mean simulation values and the lines represent fitted logistic regressions. The horizontal dotted and dashed lines represents the 5% and 1% threshold for quasi-extinction respectively. Curves generated using a logistic regression.

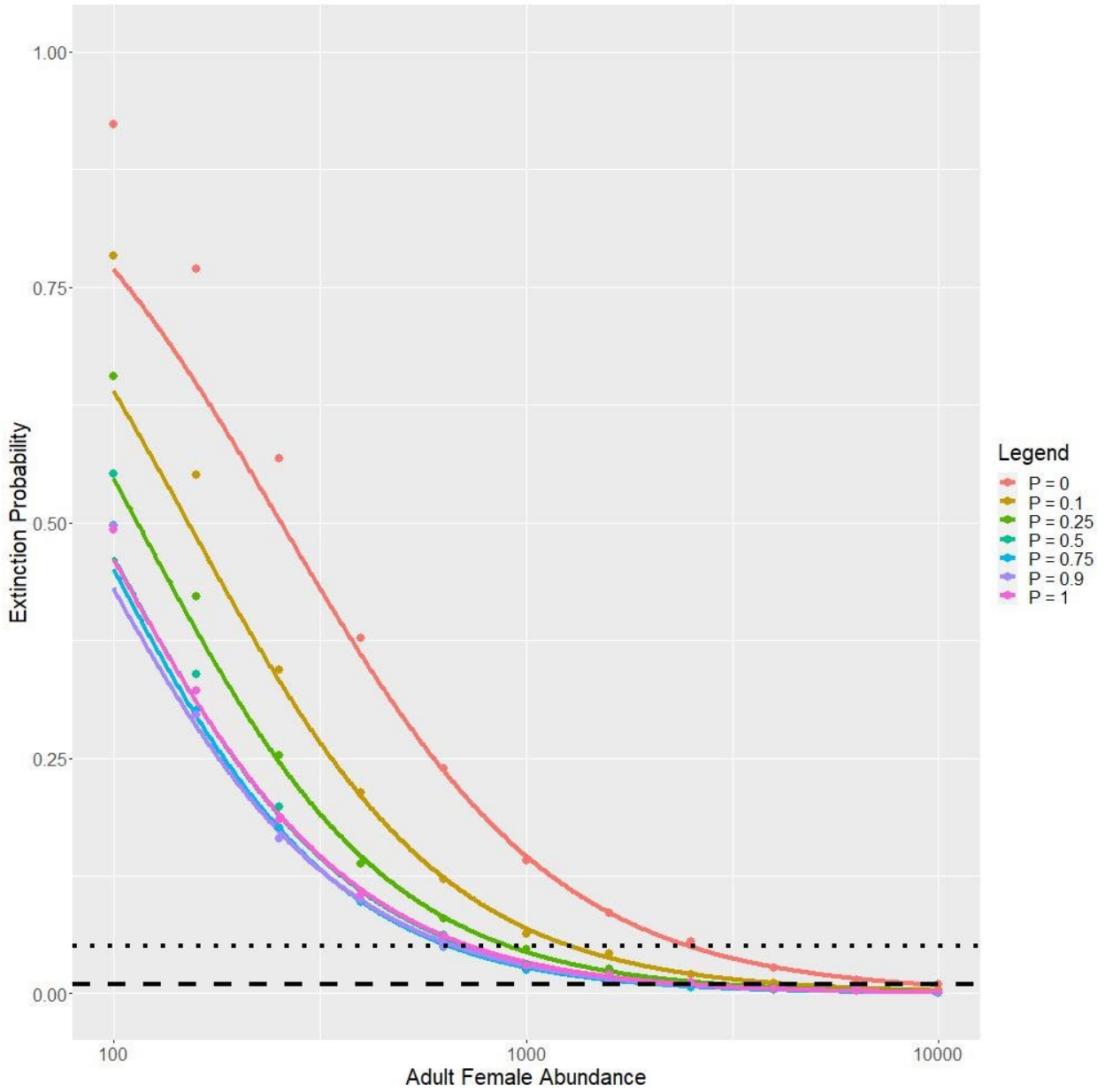

Figure 12. The probability of quasi-extinction at various adult female abundances for seven large-bodied DU proportions and at a 15% per generation catastrophe rate. The points represent mean simulation values and the lines represent fitted logistic regressions. The horizontal dotted and dashed lines represents the 5% and 1% threshold for quasi-extinction respectively. Curves generated using a logistic regression.

The frequency of catastrophes has a strong impact on the required population size for sustainability. In general, it requires 1.5 to 2 times the number of female adults to sustain the population under a 15% generational catastrophe rate compared to the 10% rate.

Under the scenario where the two DUs are reproductively isolated, the number of adult female small-bodied DU LWF required for a 99% persistence likelihood over 100 years is ~4,100 for a 10% generational catastrophe rate and ~8,700 for the 15% rate. For the large-bodied DU, the numbers required are ~1,400 and ~2,300 for 10% and 15% catastrophe rate respectively.

Under the alternative life-history scenario and depending on the proportion of large-bodied DU, the total number of adult females required is ~1,200–2,300 for the 10% catastrophe rate and ~1,900–4,200 for the 15% rate, depending on the value of *p*.

Assuming a stable age structure and based on the maturity schedule, the number of adult females can be converted to a population size comprising of both sexes and all juvenile and adult individuals. The small-bodied DU MVP is ~11,000 for a 10% generational catastrophe rate and ~24,000 for the 15% rate. The large-bodied DU MVP is ~11,000 and ~19,200 for 10% and 15% catastrophe rate respectively. Using the highest female adult estimate from the range of proportion values, the MVP for an alternative life-history population is ~8,600 and ~14,700 for 10% and 15% catastrophe rate respectively.

Habitat: Minimum Area for Population Viability (MAPV)

An OMNRF netting survey in 2010 estimated a large-bodied DU population size of 11,378 (95% CI: 6,509–18,712) and in 2019 estimated a population of 22,792 (95% CI: 10,437–54,414). Lake Opeongo has an area of 58.6 km^2 (5,860 hectare). Under the more recent population estimate, the large-bodied DU has a density of 3.9 individuals per hectare. At a density of 3.9/ha, the large-bodied DU MVP under the 15% per generation catastrophe rate requires an area of ~4,900 ha, which is less than the area of Lake Opeongo. Hence Lake Opeongo provides sufficient habitat for the large-bodied DU.

For the small-bodied DU, estimates of population or density were not available. Under the 15% catastrophe rate, a small-bodied DU MVP of ~24,000 would be equal to a density of 4.1 individuals per hectare. Since small-bodied DU density was not available from netting surveys, the density was estimated using Equation 17 with the equation's intercept adjusted to a value of 2.72 to reflect Lake Opeongo conditions. This produces a small-bodied DU density estimate of 20.1 individuals per hectare. Thus a population of 24,000 small-bodied DU would require ~1,200 hectare, which Lake Opeongo more than adequately provides.

RECOVERY TIMES

Since small-bodied DU abundance was unknown, simulations were used to estimate a time-to-recovery assuming a low current abundance. MVP was set as the carrying capacity and was used as the recovery target. Initial population was set at 10% of MVP. These simulations reflect a situation where there is an increase in available habitat or a removal of threats or competitors (e.g., Cisco) such that vital rates return to a state that permits population size increase towards carrying capacity.

Recovery simulations result in a distribution of recovery times as shown on Figure 13. Ninety-five percent of populations reached recovery in 24 years or less.

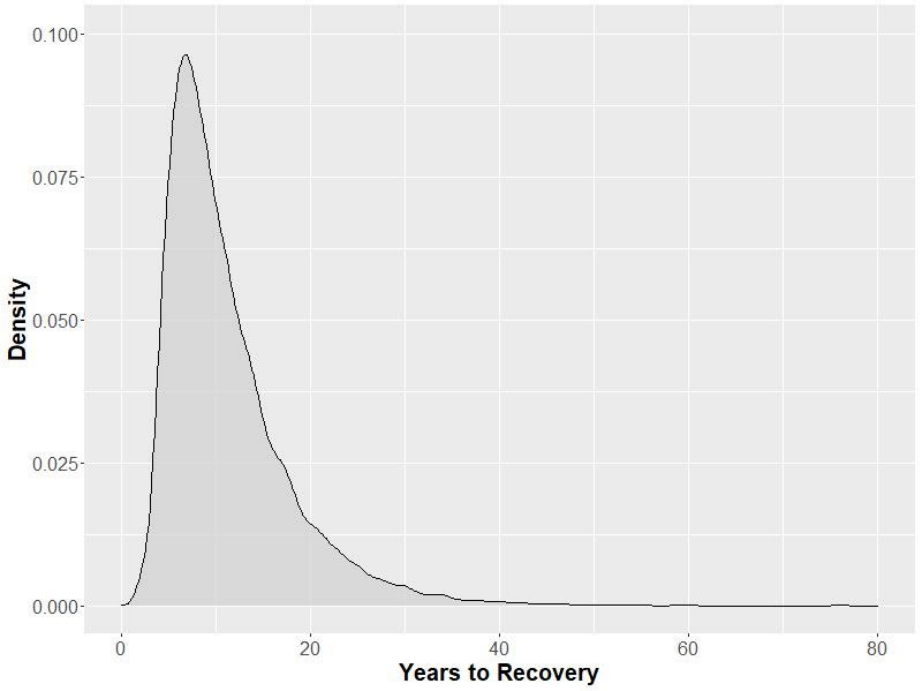

Figure 13. Distribution of recovery time-frames for all simulations of the small-bodied DU LWF given a recovery target of MVP and initial population of 10% of MVP.

DISCUSSION

A population model for the LWF species pair in Lake Opeongo was created to make predictions on how the population may respond to anthropogenic harm and estimate recovery targets for abundance and habitat. Very limited information on Lake Opeongo LWF life-history characteristics has been published. The available information was compiled and additional parameters estimated using survey data from OMNRF.

Elasticity analysis of λ and simulations were used to assess the impacts of harm to LWF populations. Both methods show LWF are generally most impacted by perturbations to the adult stage. This result holds for populations with declining or stable growth rates, but as growth rate increases, λ becomes more sensitive to the younger life stages. This pattern was observed for both the reproductively isolated model and the alternative life-history model. In addition, for the alternative life-history model, as the population growth rate increases so does λ's sensitivity to the small-bodied vital rates. The λ's sensitivity to *p* (the proportion of large-bodied individuals) also goes from positive to negative as population growth rate increases.

Simulation analysis was required to investigate the impacts of harm occurring periodically (at greater than one year intervals) as sensitivity analysis assumes all perturbations are permanent. For the reproductively isolated model, both large-bodied and small-bodied DUs experienced greater impact when harm is applied to the adult and juvenile stages. For the alternative life-history model, harm applied to the juveniles and adults of one DU will initially have a strong impact. However, as the DU being harmed is depleted, the impact to the overall population levels off. To drive the entire population to extinction, harm would need to affect the YOY stage or juveniles and adults of both DUs simultaneously.

Estimates of recovery targets for abundance were made based on simulation analysis to determine the population sizes required for demographic stability through estimates of minimum viable population size (MVP). The results depend mostly on the model used, persistence

probability and rate of catastrophe. Under the reproductively isolated model, the large-bodied DU requires ~2,300 female adults or ~19,200 adults and juveniles of both sexes to achieve 99% persistence probability under a 15% per generation catastrophe rate. The small-bodied DU requires ~8,700 female adults or ~24,000 adults and juveniles of both sexes. Under the alternative life-history model, the number of total adult females of both DUs required depends on the proportion of the two DUs and ranges from ~1,900 to ~4,200. Using the higher estimate, the MVP is ~14,700 adults and juveniles. A netting survey conducted by OMNRF in 2019 gave a population estimate of 22,792 for the large-bodied DU with a 95% confidence interval of 10,437–54,414. Therefore, the current population of the large-bodied DU is likely above the MVP. Population estimates for the small-bodied DU were not available.

Estimates of MVP were converted to habitat requirements by dividing MVP by mean estimates of density. Large-bodied DU MVP requires an area of 49 km^2. Density for the small-bodied DU was estimated to be 20.1/ha, which produces a habitat requirement of 12 km^2. Both MAPV estimates are less than the area of Lake Opeongo and thus it is likely there is sufficient habitat for LWF populations.

UNCERTAINTIES

The life history characteristics of the Opeongo LWF species pair were not well-described in the literature. As a result, there is uncertainty in the parameterization of the population model. Maturity and growth were fitted to a small data set (large-bodied DU n = 182, small-bodied DU n = 23) and limited timespan. Mortality and maximum population growth were calculated using general allometric relationships. This implicitly assumes that the differences between the large-bodied and small-bodied DUs could be attributed solely to their differences in size, longevity and maturity rate.

Fecundity was based on an older report where there was no effort made to distinguish between the DUs (Ihssen et al. 1981). However, the lengths of the fishes used in the analysis strongly suggests these belonged to the large-bodied DU. This length-fecundity relationship derived from the large-bodied DU was also applied to the small-bodied DU. If the small-bodied DU have a higher egg count than expected from the relationship, the population growth rate could be higher and the population more resilient. The DU should be expected to be more vulnerable if the egg count was lower.

Unpublished OMNRF data from the 1980s seemed to indicate the presence of individuals identified as belonging to the small-bodied DU but with longevity up to 25 years and with length greater than 200 mm. However, since these data contradicted the fish size data originally observed in Kennedy (1943) and the most recent (2010s) OMNRF data, and there was a lack of documentation on the gear and methodologies used to catch and classify these fish, the data were not used in the analysis. If the small-bodied DU do grow to a larger size and live as long as these data suggest, they should be expected to exhibit population trajectories and MVP simulation results more similar to the large-bodied DU.

The sampling gear used has poor retention rates for fishes in the small-bodied DU's size range. This prevents accurate estimation of their population size and limits the ability to assess their status.

The population structure of the species pair was uncertain hence two models were provided: a model with the DUs as reproductively isolated populations and a model with the DUs as alternative life-history strategies. Under the alternative life-history model, the proportion of large-bodied DU (p) would not be a static value as was assumed but instead be a function of intrinsic (e.g., density-dependent effects on early life growth) and extrinsic (e.g., interspecific competition) factors. A model with a dynamic value of p might produce results that differ from

those presented with a static value, particularly due to shifts in DU proportions affecting the population's sensitivity to harm. The alternative life-history model did not have a hereditary determinant of life-history strategy, but it is possible that offspring of the two DUs could exhibit different *p* values due to genetic differences.

There is indirect evidence the two DUs are reproductively isolated, however, the mechanism which keeps the two DUs reproductively isolated is unknown. If the reproductive barrier is pre-zygotic (e.g., differences in spawning timing, spawning location, mating preference, etc.) then it is possible for hybridization to occur in cases where those barriers fail due to changes in the environment or introduction of invasive species. Such hybridization could result in the amalgamation of the species pair into a single population.

The introduction of invasive species has been identified as the main threat to the persistence of both DUs in Lake Opeongo. In particular, the introduction of *Bythotrephes* and Rainbow Smelt (*Osmerus mordax*) in the near future is considered highly likely. The impact of these invasive species and the subsequent response of the Lake Opeongo LWF is unknown. The invasive species could act as a continuous impact that drives down the LWF population for multiple years or permanently changes the available niche space, leading to a quick loss of one or both DUs.

Finally, the frequency of catastrophic events for LWF was unknown and had significant impacts on estimates of MVP. Results are presented for two rates of catastrophes, however, which is most appropriate is not clear. Best practices may be to use the more conservative estimate (15% per generation) as this is close to the cross taxa average for vertebrates (Reed et al. 2003) and to buffer against uncertainty.

ELEMENTS

Element 3: Estimate the current or recent life-history parameters for LWF.

The best available data were assembled to provide life-history parameters for LWF. The value for each life-history parameter used in the modelling is presented in Table 1.

Element 12: Propose candidate abundance and distribution target(s) for recovery

Abundance targets were estimated using population viability analysis and estimates of minimum viable population (MVP). Simulations incorporated density-dependence, environmental stochasticity, and random catastrophes. Targets varied depending on the model used, desired persistence probability and catastrophe rate (Table 4). Under the isolated reproduction model, the large-bodied DU has a MVP of ~19,200 adults and juveniles and the small-bodied DU has a MVP of ~24,000 adults and juveniles. Under the alternative life-history model, the combined population has a MVP of ~14,700 adults and juveniles.

Element 13: Project expected population trajectories over a scientifically reasonable time frame (minimum 10 years), and trajectories over to the potential recovery target(s), given current LWF population dynamics parameters.

Population estimates of the large-bodied DU are available from 2010 and 2019. Data are insufficient to project population trajectory but the population estimate is currently above the MVP. Population estimate and trajectory of the small-bodied DU is unknown.

Element 14: Provide advice on the degree to which supply of suitable habitat meets the demands of the species both at present and when the species reaches the potential recovery target(s) identified in element 12.

The quantity of habitat required to support an MVP-size population of LWF with a 1% extinction probability and a catastrophe frequency of 15% per generation was estimated to be ~49 km^2 for the large-bodied DU and ~12 km^2 for the small-bodied DU. The supply of habitat in Lake Opeongo exceeds both values.

Element 15: Assess the probability that the potential recovery target(s) can be achieved under the current rates of population dynamics, and how that probability would vary with different mortality (especially lower) and productivity (especially higher) parameters.

Population estimates of the Lake Opeongo large-bodied DU indicates that it is currently above MVP.

Element 19: Estimate the reduction in mortality rate expected by each of the mitigation measures or alternatives in element 16 and the increase in productivity or survivorship associated with each measure in element 17.

No clear links have been identified between mitigation measures and Opeongo LWF mortality rates or productivity. Therefore, it is difficult to provide guidance about the effect of mitigation measures on mortality rates or productivity.

Element 20: Project expected population trajectory (and uncertainties) over a scientifically reasonable time frame and to the time of reaching recovery targets, given mortality rates and productivities associated with the specific measures identified for exploration in element 19. Include those that provide as high a probability of survivorship and recovery as possible for biologically realistic parameter values.

Without a direct link between mitigation measures and Opeongo LWF mortality rates or productivity, this information cannot be provided under mitigation scenarios. Under ideal conditions, the small-bodied DU can reach MVP 95% of the time in 24 years or less.

Element 21: Recommend parameter values for population productivity and starting mortality rates and, where necessary, specialized features of population models that would be required to allow exploration of additional scenarios as part of the assessment of economic, social, and cultural impacts in support of the listing process.

The parameter values presented in Table 1 are based on the best available data for these populations and should be used for future population modelling.

Element 22: Evaluate maximum human-induced mortality and habitat destruction that the species can sustain without jeopardizing its survival or recovery.

The impacts of harm to populations of LWF was evaluated through estimates of the elasticity of λ (Figure 4 and 5) and simulations (Figure 6, 7 and 8). Across each analysis, perturbations to the adult stage had the greatest impact to the population.

Estimates of maximum human-induced harm can be estimated from the analysis but depend on the initial condition of the population and what the final state of the population is considered allowable. Maximum harm, which is defined here as an additional mortality or proportional reduction in habitat, can be estimated as:

$$Maximum\ Harm = \frac{final\ state - initial\ state}{initial\ state} \times \frac{1}{\varepsilon \times frequency}, \quad (17)$$

Where ε, is the estimate of elasticity for the vital rate being perturbed, frequency is the number of times per year harm is applied (e.g., 0.2 represents a 5 year periodic cycle), and state is the population parameter being measured (λ). If the initial state is currently less than the acceptable final state, there is no scope for harm. The Opeongo LWF large-bodied DU is currently above the MVP but there are no current population estimates for the small-bodied DU.

REFERENCES CITED

Caswell, H. 2001. Matrix population models: construction, analysis, and interpretation. Sinauer Associates, Sunderland, MA. 722 p.

COSEWIC (Committee on the Status of Endangered Wildlife in Canada). 2018. COSEWIC assessment and status report on the Whitefish *Coregonus* spp., European Whitefish - Squanga Lake small-bodied population (*Coregonus lavaretus*), Lake Whitefish - Squanga Lake large-bodied population (*Coregonus clupeaformis*), European Whitefish - Little Teslin Lake small-bodied population (Coregonus *lavaretus*), Lake Whitefish - Little Teslin Lake large-bodied population (*Coregonus clupeaformis*), European Whitefish - Dezadeash Lake small-bodied population (*Coregonus lavaretus*), European Whitefish - Dezadeash Lake large-bodied population (*Coregonus lavaretus*), Lake Whitefish - Lake Opeongo small-bodied population (*Coregonus clupeaformis*), Lake Whitefish - Lake Opeongo large-bodied population (*Coregonus clupeaformis*), Lake Whitefish - Como Lake small-bodied population (*Coregonus clupeaformis*) and the Lake Whitefish - Como Lake large-bodied population (*Coregonus clupeaformis*) in Canada. Committee on the Status of Endangered Wildlife in Canada. Ottawa, ON. xxxix + 42 p.

DFO. 2007a. Documenting habitat use of species at risk and quantifying habitat quality. DFO Can. Sci. Advis. Sec. Sci. Advis. Rep. 2007/038.

DFO. 2007b. Revised protocol for conducting recovery potential assessments. DFO Can. Sci. Advis. Sec. Sci. Advis. Rep. 2007/039.

Gow, J.L., Peichel, C.L., and Taylor, E.B. 2007. Ecological selection against hybrids in natural populations of sympatric threespine sticklebacks. J. Evol. Biol. 20(6): 2173–2180.

Hoenig, J.M. 1983. Empirical use of longevity data to estimate mortality rates. Fish. Bull. 82: 898–903.

Ihssen, P.E., Evans, D.O., Christie, W.J., Reckhan, J.A., and DesJardine, R.L. 1981. Life history, morphology, and electrophoretic characteristics of five allopatric stocks of Lake Whitefish (*Coregonus clupeaformis*) in the Great Lakes Region. Can. J. Fish. Aquat. Sci. 38: 1790–1807.

Jonsson, B., and Jonsson, N. 1993. Partial migration: niche shift versus sexual maturation in fishes. Rev. Fish Biol. Fish. 3: 348–365.

Kenchington T.J. 2014. Natural mortality estimators for information-limited fisheries. Fish Fish. 15(4): 533–562.

Kennedy, W.A. 1943. The Whitefish, *Coregonus clupeaformis* (Mitchill), of Lake Opeongo, Algonquin Park, Ontario. On. Fish. Res. Lab. No. 62: 25 p.

Lande, R. 1988. Genetics and demography in biological conservation. Science 241(4872): 1455–1460.

Lorenzen, K. 2000. Allometry of natural mortality as a basis for assessing optimal release size in fish-stocking programmes. Can. J. Fish. Aquat. Sci. 57: 2374–2381.

Mee, J.A., Bernatchez, L., Reist, J.D., Rogers, S.M., and Taylor, E.B. 2015. Identifying designatable units for intraspecific conservation prioritization: a hierarchical approach applied to the lake whitefish species complex (*Coregonus* spp.). Evol. App. 8(5): 423–441.

Moore, J-S., Loewen, T.N., Harris, L.N. and Tallman, R.F. 2014. Genetic analysis of sympatric migratory ecotypes of Arctic charr *Salvelinus alpinus*: alternative mating tactics or reproductively isolated strategies? J. Fish Biol. 84(1): 145–162.

Morris, W.F., and Doak, D.F. 2002. Quantitative conservation biology: theory and practice of population viability analysis. Sinauer Associates, Sunderland, MA. 480 p.

Proulx, R., and Magnan, P. 2004. Contribution of phenotypic plasticity and heredity to the trophic polymorphism of lacustrine brook charr (*Salvelinus fontinalis* M.). Evol. Ecol. Res. 6: 503–522.

R Core Team, 2020. R: A language and environment for statistical computing. R Foundation for Statistical Computing, Vienna, Austria.

Randall, R.G., Kelso, J.R.M., and Minns, C.K. 1995. Fish production in freshwaters: Are rivers more productive than lakes? Can. J. Fish. Aquat. Sci. 52: 631–643.

Randall, R.G., and Minns, C.K. 2000, Use of fish production per unit biomass ratios for measuring the productive capacity of fish habitats. Can. J. Fish. Aquat. Sci. 57: 1657–1667.

Reed, D.H., O'Grady, J.J., Ballou, J.D., and Frankham, R. 2003. The frequency and severity of catastrophic die-offs in vertebrates. Anim. Cons. 6: 109–114.

Rundle, H.D., and Schluter, D. 1998. Reinforcement of stickleback mate preferences: sympatry breeds contempt. Evolution 52(1): 200–208.

Shaffer, M.L. 1981. Minimum population sizes for species conservation. BioScience 31: 131–134.

Trudel, M., Tremblay, A., Schetagne, R., and Rasmussen, J.B. 2001. Why are dwarf fish so small? An energetic analysis of polymorphism in lake whitefish (*Coregonus clupeaformis*). Can. J. Fish. Aquat. Sci. 58: 394–405.

van der Lee, A.S. and Koops, M.A. 2016. Are small fishes more sensitive to habitat loss? A generic size-based model. Can. J. Fish. Aquat. Sci. 73: 716–726.

Vélez-Espino, L.A., and Koops, M.A. 2009. Quantifying allowable harm in species at risk: application to the Laurentian black redhorse (*Moxostoma duquesnei*). Aquat. Conserv. Mar. Freshw. Ecosyst. 19(6): 676–688.

Vélez-Espino, L.A., Randall, R.G., and Koops, M.A. 2010. Quantifying habitat requirements of four freshwater species at risk in Canada: Northern Madtom, Spotted Gar, Lake Chubsucker, and Pugnose Shiner. DFO Can. Sci. Advis. Sec. Sci. Res. Doc. 2009/115. iv + 21 p.

Vélez-Espino, L.A., and Koops, M.A. 2012. Capacity for increase, compensatory reserve, and catastrophes as determinants of minimum viable population in freshwater fishes. Ecol. Model. 247: 319–326.